

УДК 621.38

Agafonov A.A.

Head department higher mathematics and mathematical modeling

Kazan (Volga Region) Federal University

Mustafoyev A.

Assistant at the Department of Radioelectronics

Jizzakh Polytechnic Institute

OPTICAL PROPERTIES OF POROUS NANO-SIZED GAAS

***Abstract:** Optical properties of a porous GaAs obtained electrochemically on n- and p-type GaAs(100) plates have been studied. The GaAs wafer doping type considerably affect nanocrystal shape, nanocrystal average diameter and chemical surface states. Comparing the reflectivity spectra of a porous GaAs with the ones of a GaAs crystal, the changes in the spectral dependences of the reflectance within the phonon resonance region may be seen. The surface morphology of porous GaAs prepared on the substrate of an n-type GaAs has been studied using the atomic-force microscopy. A nanosized contour of the porous GaAs surface was watched. Estimations of the size of nanocrystals in a porous GaAs both by the Raman and infrared spectroscopy as well as the photoluminescence and atomic-force microscopy agree well.*

***Key words:** Raman spectroscopy, thermal oxidation, nanophases, nanofilms, plasma oscillation, surface roughness, optical-phonon mode, island growth.*

Introduction

Reduced-dimensional GaAs structures, such as quantum wires and quantum dots, are attracting increasing interest both as objects of fundamental research [1, 2] and as promising materials for creating devices based on them with new operational capabilities that are impossible obtained using traditional semiconductor materials [3]. For example, the use of porous GaAs (por-GaAs)

as a substrate material when growing epitaxial GaN layers by molecular beam epitaxy made it possible to obtain continuous layers of cubic GaN modification [4]. Using gas-phase epitaxy from metal-organic compounds, single-crystal layers of GaAs, AlGaAs and InGaAs were obtained on por-GaAs substrates [5]. It seems very promising to obtain various porous semiconductor materials using the method of electrochemical etching. This method is quite simple and its implementation does not require large expenses. In case of a positive result

It will be possible to expand the spectral range of luminescent electronics, as well as create new types of LEDs. In addition, the use of porous materials as intermediate layers will make it possible to obtain new types of heterojunctions. Attempts made in this direction have shown that this problem can be successfully solved [4,6,7]. Currently, not many works are devoted to the issue of obtaining nanosized porous GaAs [2,5,8]. The information presented in them is sometimes contradictory and there is practically no information about the lattice dynamics of nanocrystals (NCs) forming a layer of porous GaAs **Samples and experimental procedure**

Raman scattering

When interpreting the Raman spectra of por-GaAs samples, it is extremely important to have information about the chemical composition of the surface of the nanocrystals. Based on the research results obtained using the X-ray photoelectron spectroscopy (XPS) method, it was concluded that in the studied samples the Ga : As ratio was ~ 1 , i.e., the stoichiometry of the material was preserved. In addition, chlorine was present on the surface, but its amount did not exceed 3 at%.

As a result of the electrochemical etching reaction on the surface of GaAs NCs, chemical compounds such as Ga_2O_3 , GaCl_3 , AsCl_3 , and As_2O_3 can be formed. A comprehensive analysis of XPS data, laser mass analysis and surface morphology (according to the results obtained using scanning electron

microscopy) allowed us to conclude that, of the entire set of listed compounds, As_2O_3 crystallites with diamond-like shape.

In the Raman spectra of a number of samples fabricated on n-type substrates, intense narrow peaks located almost equidistantly were observed.

For example in Figure 1 shows the Raman spectra of three porous n-GaAs samples. Peaks 3 and 4 present in the spectra correspond to the frequencies of transverse (ωTO) and longitudinal (ωLO) GaAs optical phonons, which are active in the Raman spectra of both crystalline and porous modifications of gallium arsenide. In the first case, these vibration modes should be located at frequencies of 268.5 cm^{-1} (TO) and 292.3 cm^{-1} (LO). In the case of por-GaAs, the Raman phonon lines are broadened and shifted to the low-frequency region of the spectrum compared to the case of a crystalline material. The authors of [1] examined the Raman spectra of the chemical compounds As_2O_3 and Ga_2O_3 in order to identify the remaining peaks numbered 1, 2, 5–7. They noticed that As_2O_3 and Ga_2O_3 did not exhibit photoluminescent properties, and in the Raman spectra of the first of them intense peaks were observed at frequencies of 85, 183, 268, 369, 414, 471 and 560 cm^{-1} . In the second case (Ga_2O_3), peaks occurred at frequencies of 201, 418, and 769 cm^{-1} . As can be seen in Fig. 1, in our case, in the spectra of a number of n-type porous GaAs samples, resonance vibrations corresponding to the As_2O_3 material are observed. No traces of Ga_2O_3 were found. From the same figure one can see that in the spectrum of sample 4-2 there is an increase in the radiation intensity at frequencies above 200 cm^{-1} . This effect is associated with the appearance of a photoluminescence (PL) signal from this sample [10]. Since no additional peaks appeared in this case, which indicates that the physicochemical state of the surface of the nanocrystals remained the same, we can conclude that the decisive role played by size quantization effects in the process of the appearance of the PL signal in the visible wavelength range in this sample. During its manufacture, the current density value was 20% higher than during the manufacture of sample

4. If we further increase the current passing through the sample during the electrochemical etching reaction, then the electropolishing mode quickly sets in, which in turn leads to a sharp decrease in the thickness of the porous film and to its complete disappearance. For p-type samples, as shown by XPS, spectrometric and SEM analysis data, the formation of As_2O_3 crystallites on the pore surface is not observed, as was the case for some porous samples.

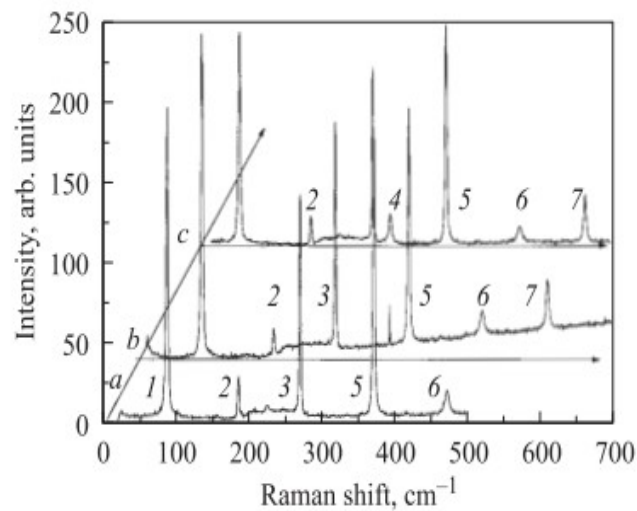


Fig. 1. Raman spectra of porous n-GaAs samples. Sample numbers: a - 2, b - 4-2, c - 4.

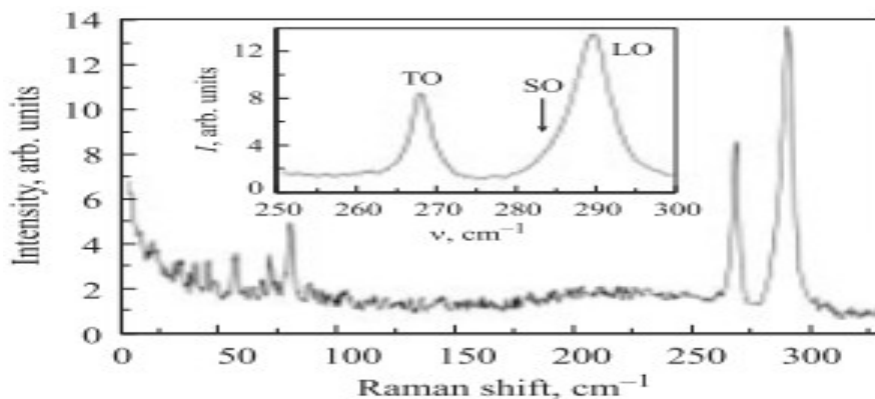


Fig. 2. Raman spectrum of the por-GaAsSi sample. The inset shows the spectral region in which TO and LO phonons appear. The arrow indicates the position of the surface optical (SO) phonon mode.

n-GaAs. At the same time, the total number of oxygen atoms involved in the formation of oxide bonds on the surface of nanocrystals turned out to be almost equal. It should be emphasized that the PL intensity in porous p-GaAs

samples is significantly lower than in porous n-GaAs samples, and the position of the PL peak itself is shifted to the red region of the spectrum [11].

The porous p-GaAs layer is less homogeneous; the NC sizes range from 10 nm to tenths of a micron. In the case of n-GaAs, the sizes of nanocrystals are smaller, as well as the dispersion of their average diameter, which was determined from the position of the PL peak maximum (E_{\max}), for which the approach outlined in [2] was used. The PL maximum in n-type por-GaAs samples was located at energies of 1.85–2.52 eV, which corresponds to NC sizes from 5 to 8 nm. Along with this, similar estimates were made based on the shift of the main optical phonons in the Raman spectra of por-GaAs, as well as using atomic force microscopy (AFM) methods. So, for example, from Fig. 2, which shows the Raman spectrum of n-type por-GaAs free of As_2O_3 , one can see that the peak corresponding to the scattering of light quanta on longitudinal optical phonons in por-GaAs is shifted by $1\omega \approx 1.6 \text{ cm}^{-1}$ to the low-frequency region of the spectrum along compared with the case of bulk gallium arsenide. Knowing the value of 1ω , one can estimate the average diameter of the nanocrystals forming the n-por-GaAs layer in this sample. As a result, the NC diameter $d \approx 5.9 \text{ nm}$ was obtained, which is consistent with

estimate made for the same sample based on PL results ($d \approx 6.3 \text{ nm}$, $E_{\max} = 2.12 \text{ eV}$). In the Raman spectra of por-GaAs samples, along with optical phonons localized in the bulk of the NC, surface optical (SO) phonon modes were detected. In order to estimate the frequencies of SO-phonon modes, a calculation was carried out within the framework of the approach described in [10]. In particular, the following relations were used to find the required frequencies:

$$\omega_{\text{SO}}^2 = \omega_{\text{TO}}^2 + \omega_p^2 \frac{\epsilon_{\infty}}{\epsilon_{\infty} + \eta_m(r)},$$

$$\eta_m(r) = -\frac{I'_m(r)K_m(r)}{I_m(r)K'_m(r)}.$$

Here r is the radius of the nanocrystal, $J_m(r)$ is the cylindrical function, ω_p is the plasma frequency, ϵ_∞ is the high-frequency dielectric constant. For the por-GaAs sample, the Raman spectrum of which is presented in

Fig. 2, the frequency of the surface phonon mode turned out to be equal to $\omega_{SO} = 284 \text{ cm}^{-1}$ (the SO mode is marked in the inset with an arrow). This value was obtained using the procedure of decomposing the LO peak into its constituent Gaussians. For the calculation, the following values of the GaAs material parameters were used: $\epsilon_\infty = 11.2$, $\omega_{TO} = 268.5 \text{ cm}^{-1}$ [11], $d \approx 6 \text{ nm}$. The theoretical estimate for ω_{SO} practically coincides with the found value.

Conclusion

The paper describes the process of obtaining layers of porous GaAs using the electrochemical etching method and presents the results of studies of their optical and structural properties. It has been shown that the morphology of the por-GaAs layer, the surface states and the size of the nanocrystals that make up the porous layer significantly depend on the type of conductivity of the initial single-crystal GaAs. In the infrared optical spectra and Raman spectra, both a shift in the peaks of the main optical phonons and the appearance of vibrational modes localized in the bulk of the NC, as well as surface phonons, were detected. An explanation is given for the complex structure of the FTIR spectra of por-GaAs. It is shown that in n-type por-GaAs samples the appearance of a PL signal in the visible region of the spectrum is due to quantum-size effects. Using AFM and XPS methods, studies of the morphology of por-GaAs and the chemical composition of nanocrystals were carried out. It was found that the stoichiometry of the NC composition is preserved, and there is also a uniform nanorelief of por-GaAs surfaces obtained on n-type gallium arsenide substrates, which may be important for their further use as a substrate material for obtaining GaAs epitaxial layers with improved structural properties. Based on the results of Raman spectroscopy, it is possible to monitor the presence of As_2O_3 and Ga_2O_3 oxides on the NC surface [12]. The values of the average

diameter of GaAs nanocrystals forming the por-GaAs layer, obtained from the results of Raman spectroscopy, FTIR, PL and AFM, are in good agreement with each other.

Reference

1. Zhabbor, M., Matluba, S., & Farrukh, Y. (2022). STAGES OF DESIGNING A TWO-CASCADE AMPLIFIER CIRCUIT IN THE “MULTISIM” PROGRAMM. *Universum: технические науки*, (11-8 (104)), 43-47.
2. Suyarova, M. (2024). ELEKTR KABELLARGA NISBATAN OPTIK TOLALI ALOQA LINIYALARINING ASOSIY AFZALLIKLARI. *Илм-фан ва та'лим*, 2(1 (16)).
3. Саттаров, С. А., & Омонов, С. Р. У. (2022). ИЗМЕРЕНИЯ ШУМОПОДОБНЫХ СИГНАЛОВ С ПОМОЩЬЮ АНАЛИЗАТОРА СПЕКТРА FPC1500. *Universum: технические науки*, (11-3 (104)), 17-20.
4. Muldanov, F. R. (2023). VIDEOTASVIRDA SHAXS YUZ SOHALARINI SIFATINI OSHIRISH BOSQICHLARI.
5. Метинкулов, Ж. (2023). ИСПОЛЬЗОВАНИЕ МИКРОКОНТРОЛЛЕРОВ ДЛЯ УПРАВЛЕНИЯ НАПРЯЖЕНИЕМ. SCIENTIFIC APPROACH TO THE MODERN EDUCATION SYSTEM, 2(20), 149-156.
6. Мулданов, Ф. Р., & Иняминов, Й. О. (2023). МАТЕМАТИЧЕСКОЕ, АЛГОРИТМИЧЕСКОЕ И ПРОГРАММНОЕ ОБЕСПЕЧЕНИЕ СОЗДАНИЯ СИСТЕМЫ РОБОТА-АНАЛИЗАТОРА В ВИДЕОТЕХНОЛОГИЯХ. *Экономика и социум*, (3-2 (106)), 793-798.
7. Islomov, M. (2023). CALCULATION OF SIGNAL DISPERSION IN OPTICAL FIBER. *Modern Science and Research*, 2(10), 127-129.

8. Irisboev, F. (2023). THE INPUTS ARE ON INSERTED SILICON NON-BALANCED PROCESSES. *Modern Science and Research*, 2(10), 120-122.

9. Якименко, И. В., Каршибоев, Ш. А., & Муртазин, Э. Р. (2023). СПЕЦИАЛИЗИРОВАННОЕ МАШИННОЕ ОБУЧЕНИЕ ДЛЯ РАДИОЧАСТОТ. *Экономика и социум*, (11 (114)-1), 1196-1199.

10. Ирисбоев, Ф. Б., Эшонкулов, А. А. У., & Исломов, М. Х. У. (2022). ПОКАЗАТЕЛИ МНОГОКАСКАДНЫХ УСИЛИТЕЛЕЙ. *Universum: технические науки*, (11-3 (104)), 5-8.

11. Бобонов, Д. Т. (2022). НАНОЭЛЕКТРОНИКА, НАНОМАТЕРИАЛЫ, НАНОТЕХНОЛОГИИ, ФОРМИРОВАНИЕ ПРЕДМЕТНОЙ ОБЛАСТИ, СТРУКТУРИРОВАНИЕ. *Involta Scientific Journal*, 1(3), 81-87.

12. Умаров, Б. К. У., & Хамзаев, А. И. У. (2022). КИНЕТИКА МАГНЕТОСОПРОТИВЛЕНИЯ КРЕМНИЯ С МАГНИТНЫМИ АНОКЛАСТЕРАМИ. *Universum: технические науки*, (11-3 (104)), 21-23.

13. Mirzaev, U., Abdullaev, E., Kholdarov, B., Mamatkulov, B., & Mustafoev, A. (2023). Development of a mathematical model for the analysis of different load modes of operation of induction motors. In *E3S Web of Conferences* (Vol. 461, p. 01075). EDP Sciences.